PERGAMON

International Journal of Heat and Mass Transfer 43 (2000) 1103–1111

International Journal of HEAT and MASS TRANSFER

www.elsevier.com/locate/ijhmt

Experimental investigation of laminar mixed convection in an inclined semicircular duct under buoyancy assisted and opposed conditions

A.A. Busedra, H.M. Soliman*

Department of Mechanical and Industrial Engineering, University of Manitoba, Winnipeg, Manitoba, Canada R3T 5V6

Received 4 January 1999; received in revised form 11 June 1999

Abstract

Combined free and forced convection is experimentally investigated for laminar water flow in the entrance region of a semicircular duct with upward and downward inclinations within $\pm 20^\circ$ using the boundary condition of uniform heat input axially. The experiment was designed for determining the effect of inclination (particularly the downward) on the wall temperature, and the local and fully-developed Nusselt numbers at three Reynolds numbers (500, 1000, and 1500) and a wide range of Grashof numbers. For the upward inclinations, Nusselt number was found to increase with Grashof number and the inclination angle (up to 20°), while the effect of Reynolds number was found to be small. For the downward inclination, Reynolds number has a strong effect on Nusselt number and the manner by which it varies with Grashof number. The fully-developed values of Nusselt number agree well in magnitude and trend with theoretical results recently obtained by the authors. © 2000 Elsevier Science Ltd. All rights reserved.

Keywords: Laminar mixed convection; Developing and fully developed; Experimental; Semicircular ducts; Inclined; Buoyancy assisted and opposed

1. Introduction

Several applications in the area of heat transfer involve mixed free and forced convection in ducts of various cross-sections and orientations. Examples of these applications include solar energy systems, cooling of electronic devices, compact heat exchangers and the cooling core of nuclear reactors. Free convection can aid the forced flow or act in opposition to it. Knowledge of the heat-transfer characteristics under both conditions can guide the design of devices used in these applications.

The present study is concerned with the experimental investigation of laminar mixed convection in a heated semicircular duct with upward (buoyancy aiding) and downward (buoyancy opposed) inclinations. Little prior work have dealt experimentally with laminar mixed convection in inclined ducts, particularly under buoyancy opposed conditions. Barozzi et al. [1] reported experimental data of heat transfer in horizontal and upwardly inclined circular tubes for the range $200 \leq Re \leq 2300$, $6 \times 10^3 \leq Gr \leq 7 \times 10^5$ and $0 \leq \alpha \leq 60^\circ$. They noted that the local Nusselt number first decreases along the heated length, reaches a minimum, and then increases to the fully-developed value. The

* Corresponding author. Tel.: +1-204-474-9307; fax: +1-204-275-7507.

E-mail address: hsolima@cc.umanitoba.ca (H.M. Soliman).

0017-9310/00/$ - see front matter © 2000 Elsevier Science Ltd. All rights reserved.
PII: S0017-9310(99)00208-2

Nomenclature

A_{fl}	cross-sectional flow area defined by Eq. (2) (m^2)
C_p	specific heat (J kg^{-1} K^{-1})
D_h	hydraulic diameter defined by Eq. (2) (m)
g	gravitational acceleration (m s^{-2})
Gr	Grashof number defined by Eq. (1)
h	convective heat transfer coefficient (W m^{-2} K^{-1})
k	thermal conductivity (Wm^{-1} K^{-1})
$\dot{m}$	mass flow rate (kg s^{-1})
Nu	Nusselt number
Pr	Prandtl number ($= \mu C_p/k$)
q'	heat input per unit length (W m^{-1})
r_0	radius of the circular part of the duct (m)
Re	Reynolds number
T	temperature (K)
Z	axial coordinate measured from the beginning of heating (m)
Z^+	dimensionless axial coordinate ($= Z/D_h RePr$)
α	inclination angle (degrees)

Greek symbols

β	coefficient of thermal expansion (K^{-1})
μ	viscosity (N s m^{-2})
ρ	density (kg m^{-3})

Subscripts

a, b, c	thermocouple positions at an axial station
bulk	bulk value
fd	fully-developed value
m	evaluated at the mean bulk temperature
z	axially local value

Superscript

–	average value

minimum is due to a balance between entrance and free-convection effects. Variation of Nusselt number with α was found to be very small, probably due to the small values of Gr used in the study. Morcos et al. [2] investigated the circumferential variation of wall temperature and the axial variation of Nusselt number in upwardly inclined heated ducts of rectangular cross-sections. They reported that the upper wall temperatures are higher than the lower wall temperatures as a result of the secondary flow current. The axial variation of the local Nusselt number was similar to that reported in Ref. [1] and Nusselt number was found to increase with Gr and with the inclination angle up to a maximum near $\alpha = 30^\circ$. Bohne and Obermeier [3] considered the geometry of a concentric annulus with the inner tube heated electrically. They reported data for the average Nusselt number over the whole heated length in the horizontal, vertical (upward and downward flow) and inclined (upward and downward flow) orientations. Both laminar and turbulent flows were considered. Their results indicate that for upward and downward laminar flows, the average Nusselt number may increase or decrease with α depending on the values of Gr and Re. The effects of α, Re, and Gr on the wall temperature and the local Nusselt number were not examined. A detailed experiment was reported by Maughan and Incropera [4] for laminar air flow between parallel plates (30.5×308 mm cross-section) heated uniformly from below. They used the horizontal and upward inclinations up to $\alpha = 30^\circ$. The reported variation of the local Nusselt number along the heated length is similar in trend to the ones reported in Refs. [1,2]. Also, the data show that the local Nusselt number increases with both Gr and α. Lavine et al. [5] reported a visual study of flow reversal during opposing mixed convection in an inclined pipe for Re between 100 and 3500 and α from 0 to -80°. It was observed that flow reversals started from a region downstream of the heated section and extended to some upstream location that depended on α, Re, and Gr. The flow reversal length was found to be an increasing function of Gr and α and a decreasing function of Re. For the cross-section of a semicircular duct, the only available experimental data correspond to the horizontal orientation [6]. Several other investigations (not reviewed here) have dealt experimentally with laminar mixed convection in horizontal and vertical ducts.

It can be noted from the above review that ducts of various cross-sections (circular, rectangular, concentric annulus, and parallel plates) have been used in Refs. [1–4]. It is because laminar flow heat transfer, particularly in the mixed-convection mode, is strongly dependent on duct geometry and, therefore, results of one duct geometry would not apply to other geometries. The semicircular cross-section is applicable to tubes with tape inserts and multipassage tubes. No experimental results are available yet for laminar mixed convection in inclined semicircular ducts. Therefore, the present investigation was designed to examine the effects of buoyancy (both aiding and opposed) on laminar heat transfer in the thermal entrance region of an inclined semicircular duct. These effects are to be examined over a range of the independent parameters

α, Re, and Gr. The measured parameters include the axial and circumferential variation of wall temperature, the local mean Nusselt number, and the fully-developed Nusselt number. Values of Nu_{fd} are to be compared with the recent theoretical results obtained by the present authors [7].

2. Experimental apparatus and procedure

2.1. Flow loop

The test facility used in this experimental investigation is shown in Fig. 1. Distilled water (used as the working fluid) was circulated around the loop by a centrifugal pump. The flow rate through the test section was regulated by a by-pass line around the pump and a filter was installed upstream of the test section. The test section was mounted on a rigid beam which was pivoted at the centre to allow for inclination. The flat face of the semicircular duct was oriented vertically throughout the experimental program. Following the test section, the outlet bulk temperature was measured in a mixing chamber. The test fluid was then cooled in one or two heat exchangers and its flow rate was measured by variable-area type flowmeters before returning it to the accumulating tank.

2.2. Test section

The semicircular test section was constructed using type K copper tubing (49.8-mm i.d. and 54.0-mm o.d.) and brass plates (3.2 mm thick). The test section consisted of three parts: a hydrodynamic developing length of 2.7 m, a heated length of 4.7 m and an outlet length of 0.3 m. The heat input (in the heated section) was generated by flat electric resistance wires with a total resistance of 6.85 Ω. The heated section was first covered by an electrical insulating varnish coating and then wrapped by a layer of fibre glass insulating tape to protect the varnish from the heater wires. Two wires were carefully wound in parallel and with a uniform pitch. The resistance of the twin heaters was axially uniform to within 5%. The heating wires were then covered with high-temperature, high-thermal-conductivity cement to ensure that the wires remained firmly in place at all operating temperatures and also to uniformly distribute the input heat. The input power was regulated by an AC power variac and measured by a digital Watt-meter. The whole test section was covered by a 5-cm thick layer of fibre glass thermal insulation. Heat loss through the insulation was measured by a heat flux meter (HEATPROBE, model HA-100) and was found to be within 3% of the total heat input. The measured heat loss by the heat flux meter was used in adjusting the electrical power input.

Wall temperatures were measured at 19 axial locations within the heated section with three thermocouples (a, b, and c) at each location, as shown in Fig. 1. The axial distance between wall thermocouples varied from 100 mm at the beginning of the heated sec-

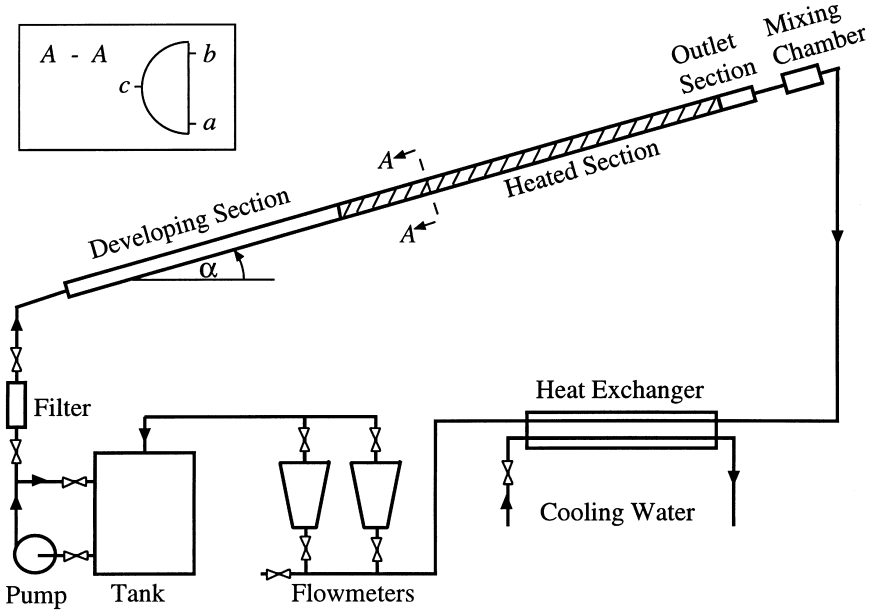

Fig. 1. Experimental flow loop.

tion, to 300 mm in the middle section, down to 200 mm in the last five stations. The inlet bulk temperature was measured at the beginning of the hydrodynamic developing length and the measured axial gradient of wall temperature at the beginning of heating was used to correct this value. A similar procedure was used in correcting the outlet bulk temperature. A straight line was fitted between the inlet and outlet bulk temperatures.

2.3. Procedure and data reduction

The three independent parameters in this experiment are Reynolds number (controlled by the flow rate), Grashof number (controlled by the input power) and the inclination angle. After adjusting the desired values of these parameters, the experiment was allowed to run for at least 4 h before steady-state conditions were achieved. When steady state was established, the readings of all thermocouples, flow meters, the input power, and the flux meter (for heat losses through the insulation) were recorded. The rate of heat gain by the test fluid was then calculated and compared with the electrical power input. The maximum deviation between these two heat rates was found to be within $\pm 6\%$ for all test runs. Actually, the heat balance error was within $\pm 3\%$ for 84% of the test runs.

The dimensionless independent parameters Re and Gr were calculated from the measured quantities using the following definitions:

$$Re = \frac{\dot{m} D_{\mathrm{h}}}{\mu A_{\mathrm{fl}}} \quad \text{and} \quad Gr = \frac{\beta g \rho^2 q' r_0^3}{\mu^2 k} \tag{1}$$

where q' is the heat input per unit length. The hydraulic diameter D_{h} and the cross-sectional flow area are given by:

$$D_{\mathrm{h}} = \frac{2\pi r_0}{\pi + 2} \quad \text{and} \quad A_{\mathrm{fl}} = \frac{\pi r_0^2}{2} \tag{2}$$

All fluid properties in Eq. (1) were calculated at the average of the inlet and outlet bulk temperatures, which is indicated by the subscript m for Re_m and Gr_m in the following sections.

The local Nusselt number was calculated from the following definition:

$$Nu_{z,i} = \frac{h_{z,i} D_{\mathrm{h}}}{k} = \frac{q' D_{\mathrm{h}}}{r_0(\pi + 2)k\left(T_{z,i} - T_{z,\mathrm{bulk}}\right)} \tag{3}$$

where i refers to wall thermocouple positions a, b, and c, as shown in Fig. 1. The local average Nusselt number at each axial station was calculated in two ways: (i) by determining the length-mean average of $Nu_{z,a}$, $Nu_{z,b}$, and $Nu_{z,c}$, and (ii) by determining the length-mean average $\bar{T}_{z,i}$ of the three wall temperatures and then using Eq. (3) for the local mean Nusselt number. The two values obtained from (i) and (ii) were very close and, therefore, the local mean Nusselt number was taken as the average of these two values [6], i.e.,

$$Nu_z = \frac{\left[\dfrac{\bar{h}_{z,i} D_{\mathrm{h}}}{k} + \dfrac{q' D_{\mathrm{h}}}{r_0(\pi + 2)k\left(\bar{T}_{z,i} - T_{z,\mathrm{bulk}}\right)}\right]}{2} \tag{4}$$

The value from Eq. (4) will be called 'the local Nusselt number' in the following sections without using the word 'mean' for briefness.

The uncertainty bounds were estimated for all the local values of Re, Gr, and Nu for all 89 test runs using the method outlined by Kline and McClintock [8] and Moffat [9]. A summary of the results for all test runs is given in the following paragraph.

The uncertainty in Re was found to be within $\pm 3.5\%$ for all test runs. The uncertainty in α was estimated to be within $\pm 0.2^\circ$. The uncertainty in Gr and Nu was found to be dependent on the values of Re and Gr. As Re increased and/or Gr decreased, the uncertainty in Nu and Gr was found to increase. The reason is that high Re (i.e., high water flow rate) and low Gr (i.e., low heat input) would result in low temperature differences between the wall and the bulk, and between outlet bulk and inlet bulk. For example, at $\alpha = 0^\circ$, $Re_m = 1000$, and $Gr_m = 1.06 \times 10^8$, the uncertainty in Gr is within $\pm 8.4\%$ and the uncertainty in Nu is within $\pm 5.4\%$. These uncertainties are higher for $\alpha = 0^\circ$, $Re_m = 1500$, and $Gr_m = 4.58 \times 10^6$, where the uncertainty in Gr is within $\pm 19.1\%$ and the uncertainty in Nu is within $\pm 26.5\%$. The highest uncertainties were found at $\alpha = 0^\circ$, $Re_m = 1500$, and $Gr_m = 2.36 \times 10^6$, where the uncertainty in Gr was found to be within $\pm 33\%$ and the uncertainty in Nu to be within $\pm 42\%$.

3. Experimental results and discussion

A total of 89 test runs were conducted in this investigation covering the following ranges of the independent parameters:

$Re_m = 500$, 1000, and 1500
$Pr_m = 4.6$–6.5 (water)
$Gr_m = 1.54 \times 10^6$–1.15×10^8
$\alpha = 20^\circ$, 10°, 0, -10°, and -20°

A different range of Gr_m was covered for each combination of α and Re_m. For example, at $\alpha = -20^\circ$ and $Re_m = 500$, it was not possible to go beyond $Gr_m = 8.61 \times 10^6$ due to oscillations in thermocouple readings indicating flow instabilities. In general, the maximum Gr_m for which steady readings were possible increased

as Re_m increased, and was much higher for upward inclinations than for downward inclinations.

3.1. Wall temperature

Results of the wall-temperature measurement for $\alpha = 0°$and $Re_m = 1000$ are shown in Fig. 2 for four values of Gr_m. The circumferential variation of wall temperature at each axial station is indicated by the readings of the three thermocouples a, b, and c (see Fig. 1 for locations), and the slope of the bulk temperature is shown for each Gr_m. Fig. 2 shows that the circumferential variation of wall temperature increases as Gr_m increases. The trend in these results is that $T_{z,b} > T_{z,c} > T_{z,a}$. This trend is consistent with the physics of the problem whereby the cross-sectional secondary flow current pushes the heavier (cooler) fluid towards the bottom of the cross-section, while the lighter (warmer) fluid rises [2]. For each Gr_m, a fully-developed region is reached where the wall and bulk temperatures appear to be increasing at the same linear rate with Z. Similar trends were noted for all data of the horizontal orientation ($Re_m = 500$ and 1500).

A representative sample of the results for upward inclinations is shown in Fig. 3 using the data for $\alpha = 20°$ and $Re_m = 1000$. These data show similar trends as those seen in Fig. 2 (i.e., $T_{z,b} > T_{z,c} > T_{z,a}$, and the circumferential variation of wall temperature increasing with Gr_m). However, comparing results of similar Gr_m (e.g., $Gr_m = 1.06 \times 10^8$ in Fig. 2 and $Gr_m = 1.01 \times 10^8$ in Fig. 3), we notice that the magnitude of circumferential variation is lower for upward inclinations than the horizontal orientation. This can be attributed to the fact that only a component of the net body force is

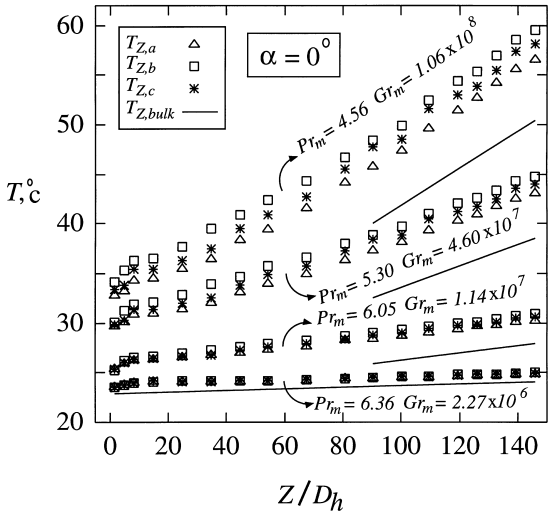

Fig. 2. Variation of wall temperature for $Re_m = 1000$ and $\alpha = 0$.

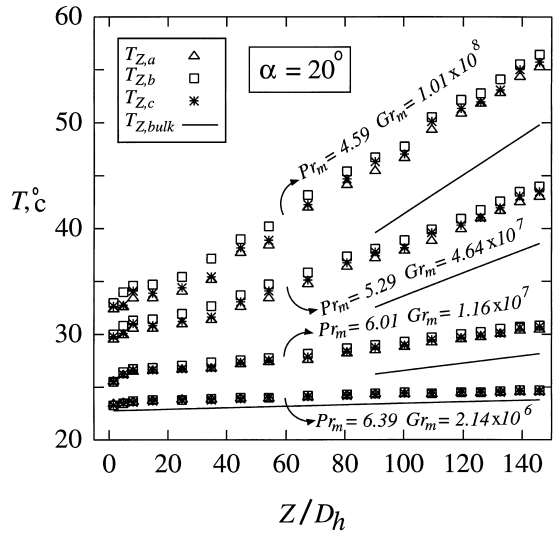

Fig. 3. Variation of wall temperature for $Re_m = 1000$ and $\alpha = 20°$.

driving the cross-sectional secondary flow due to inclination, resulting in a weaker secondary flow current and less circumferential variation of wall temperature.

For the downward inclination, the net body force has two components; one normal to the main flow direction (driving the secondary flow within the cross-section), and the other component acts opposite to the main flow direction. The second component would influence the velocity and temperature profiles in the heated section and may give rise to flow reversal in the upper part of the cross-section at high Gr_m and low Re_m [5]. Fig. 4 shows the temperature development for $\alpha = -20°$, and $Re_m = 500$ and 1500. For $Re_m = 1500$, and Gr_m up to 1.12×10^7, the wall temperature development looks similar to the horizontal and upward inclinations. It was not possible to extend Gr_m to higher values due to temperature oscillations. For $Re_m = 500$, the component of adverse net body force has a much stronger influence on the development of the hydrodynamic and thermal boundary layers as evidenced by the wall-temperature distribution. The wall-to-bulk temperature difference is large at the beginning of heating and it decreases continuously along the heated length without reaching fully developed conditions for $Gr_m > 5 \times 10^6$. In a recent theoretical analysis by the authors [7], it was found that flow reversal starts at $Gr = 2 \times 10^6$ under the present conditions of α, Pr and Re. Therefore, it is postulated that the temperature distribution shown in Fig. 4 for $Re_m = 500$ is due to a flow reversal current moving hot fluid from the end of the heated section backward towards the beginning of the heated section.

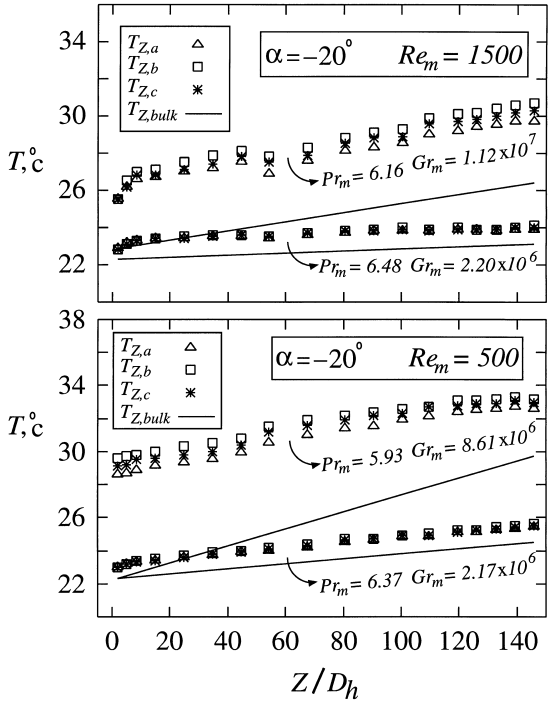

Fig. 4. Variation of wall temperature for $\alpha = -20^\circ$.

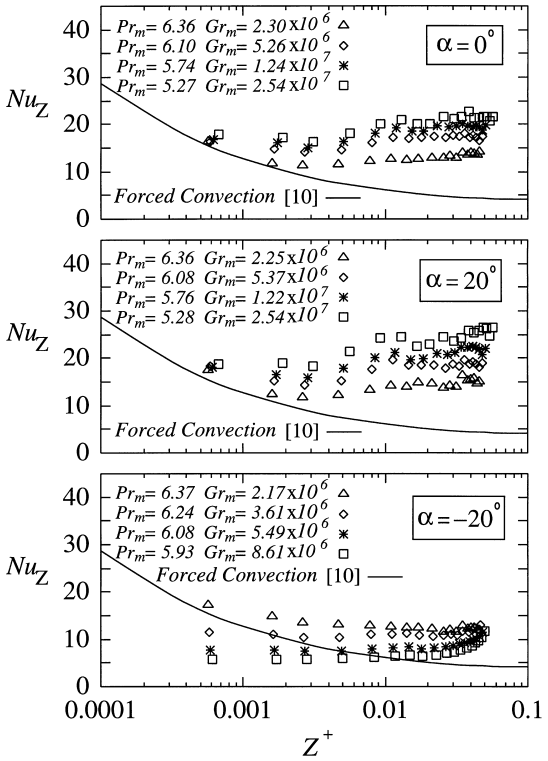

Fig. 5. Effect of inclination on Nu_z for $Re_m = 500$ (for forced convection see Ref. [10]).

3.2. Local Nusselt number

Results of the local Nusselt number, Nu_z, are presented in Figs. 5–7 in a manner that can illustrate the effects of the independent parameters Gr_m, α, and Re_m. Fig. 5 corresponds to $Re_m = 500$, $\alpha = 0$, 20°, and -20°, and the widest possible range of Gr_m. For $\alpha = 0$, Nu_z is close to the forced-convection value at low Z^+, decreses to a minimum as Z^+ increases, and then rises due to the effect of free convection before reaching a nearly constant (fully developed) value. This behaviour is similar to the one noted by Maughan and Incropera [4] and Lei and Trupp [6]. It is also clear that Gr_m has a strong effect on Nu_z, whereby Nu_z increases significantly with Gr_m in both the developing and the fully-developed regions. For the upward inclinations (represented by $\alpha = 20^\circ$ in Fig. 5), the axial variation of Nu_z is similar to the horizontal orientation. However, for nearly the same values of Gr_m, values of Nu_z are slightly higher for the upward inclination in both the developing and the fully-developed regions. This is because the net body force has a component in the axial flow direction which accelerates the fluid resulting in an increase in the heat transfer coefficient. Again, this trend is consistent with the results of Maughan and Incropera [4]. However, for downward inclinations (represented by $\alpha = -20^\circ$ in Fig. 5), the component of the net body force acts opposite to the axial flow direction, thus retarding the flow and possibly causing flow

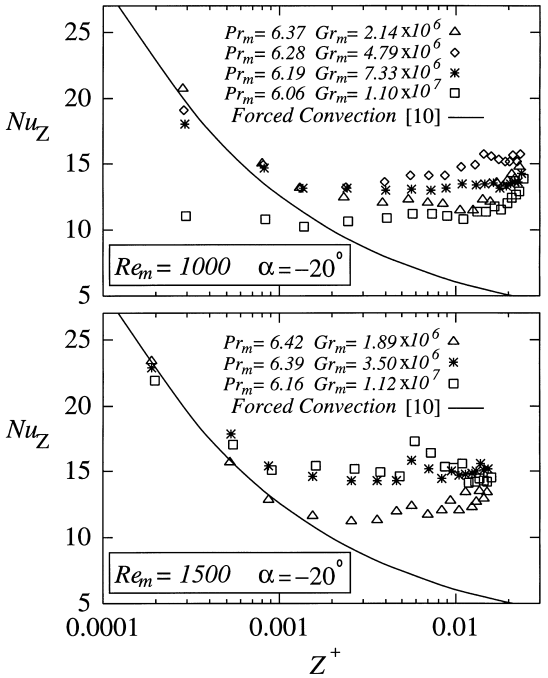

Fig. 6. Effect of Re_m on Nu_z for $\alpha = -20^\circ$ (for forced convection see Ref. [10]).

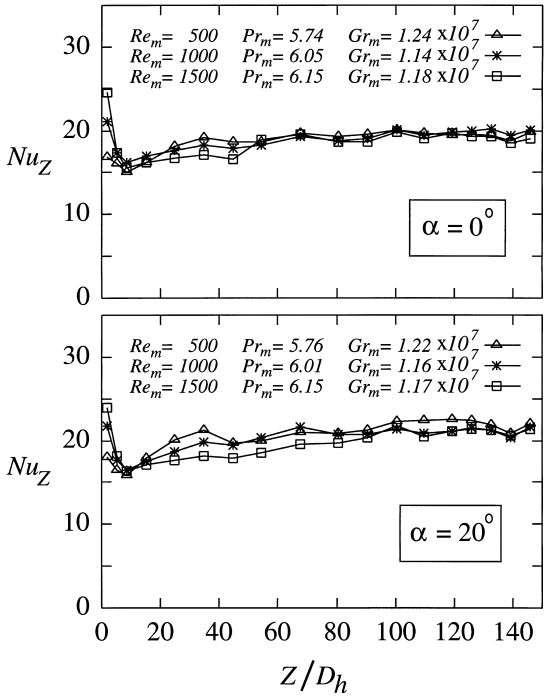

Fig. 7. Effect of Re_m on Nu_z for $\alpha = 0$ and 20°.

reversal in the upper part of the cross-section. For large Gr_m, this axial secondary flow loop may extend over most of the heated section causing significant effects on the velocity and temperature profile. Under these conditions, Fig. 5 shows that Nu_z decreases continuously with Gr_m to the degree that values lower than the forced-convection value are encountered in the developing region. At high Gr_m, the flow does not reach fully-developed conditions with Nu_z increasing continuously with Z^+.

The behaviour of Nu_z for downward inclinations was found to be very sensitive to the value of Re_m. This is illustrated in Fig. 6 for $\alpha = -20^\circ$ using $Re_m =$ 1000 and 1500 (data for $Re_m = 500$ are in Fig. 5). In all cases, the net body force acts to retard the flow; however, the effect on heat transfer depends on the mean velocity of the flow. For $Re_m = 1500$, there is enhancement in heat transfer as Gr_m increases from 1.89×10^6 to 3.50×10^6. However, a further increase in Gr_m from 3.50×10^6 to 1.12×10^7 resulted in very small change in heat transfer. For $Re_m = 1000$, values of Nu_z start out increasing with Gr_m up to a maximum followed by a decrease in Nu_z with further increase in Gr_m. This is consistent with the reasoning that when the adverse buoyancy effect gets strong enough to cause a flow-reversal region within the cross-section, the heat-transfer performance begins declining. This reasoning is consistent with the theoretical results in [7]. As Re_m decreases, the value of Gr_m at which Nusselt number begins declining decreases, as evidenced by the results for $Re_m = 500$.

Typical results on the effect of Re_m on Nu_z for the horizontal and upward inclinations are shown in Fig. 7 using Gr_m of about 1.2×10^7 and the three values of Re_m. Early in the developing region ($Z/D_h < 8$), where forced convection is dominant, we note that Nu_z increases slightly with Re_m. In this region, Nu_z decreases with Z for all Re_m due to the thickening of the boundary layer. As the wall-to-bulk temperature difference increases, free convection becomes significant and Nu_z starts increasing with Z beyond $Z/D_h = 8$. It can be noted that the rate of increase of Nu_z with Z increases as Re_m decreases. This is a logical behaviour since the impact of free convection is expected to be stronger for slower flows. Beyond a certain value of Z/D_h, the value of Nu_z becomes nearly constant (fully developed) and the effect of Re_m on Nu_z is fairly small in this region. These observations are consistent with the results in Ref. [4] for horizontal and upwardly inclined parallel plates. It is also fair to state that the effect of Re_m on Nu_z for the horizontal and upward inclinations is certainly much less significant than that for downward inclinations.

3.3. Fully-developed Nusselt number

Fully-developed conditions were established in all test runs in the horizontal and upward inclinations, as well as most test runs in the downward inclinations (except those runs of high Gr_m and low Re_m). Figs. 5–7 showed some fluctuations in Nu_z in the fully-developed region which may be attributed to property variations and buoyancy-induced fluctuations. Values of Nu_{fd} were calculated as the length-mean average of Nu_z of the six stations preceding the last station in the heated section.

The experimental values of Nu_{fd} for all values of α and Re_m are presented in Fig. 8 and lines of least-squares fit are drawn through the data. Judging by the amount of scatter in the data of $\alpha = 0$, 10°, and 20°, it may be concluded that Re_m has a small effect on Nu_{fd} for these orientations. Also, going from $\alpha = 0$ to 10°, there is a noticeable increase in Nu_{fd} at high values of Gr_m. The value of Nu_{fd} continues to increase with inclination, but at a slower rate, as α increases from 10° to 20°. Keeping in mind that for the forced-convection case, $Nu_{fd} = 4.089$ [11], we can see that free convection can enhance Nu_{fd} by a factor of up to 8 for $0 \le \alpha \le 20^\circ$.

For the downward inclinations of $\alpha = -10^\circ$ and -20°, Fig. 8 shows that Nu_{fd} is strongly dependent on Re_m. For any combination of α and Re_m, Nu_{fd} appears to follow the correlation curve for $\alpha = 0$ up to a certain value of Gr_m, where Nu_{fd} for the downward inclination starts deviating, reaches a maximum and then starts dropping with further increase in Gr_m. The value

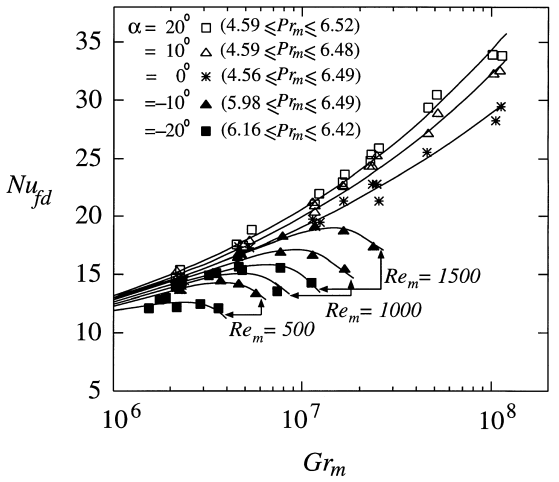

Fig. 8. Experimental results of Nu_{fd}.

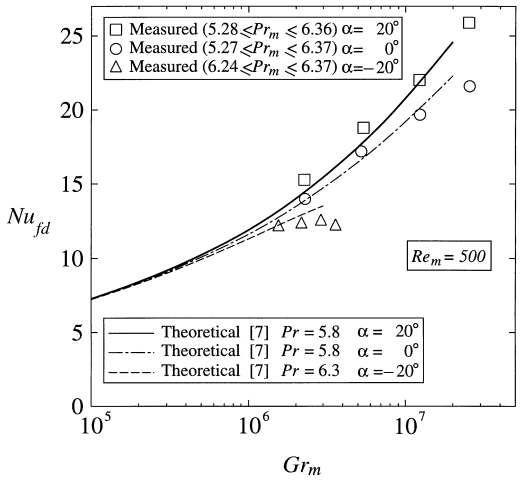

Fig. 10. Comparison between the present data for $Re_m = 500$ and the theoretical predictions in Ref. [7], $\alpha = -20°$, 0, and 20°.

of Gr_m at which this deviation occurs increases with Re_m, but decreases with $|\alpha|$.

All the trends discussed above for the upward and downward inclinations are consistent with the theoretical results reported in Ref. [7]. As a further confirmation, quantitative comparisons were made between the present experimental results and the theory in Ref. [7]. These comparisons, shown in Fig. 9 for $\alpha = 0°$ over the whole range of Re_m and in Fig. 10 for $Re_m = 500$ over the whole range of α, demonstrate very good agreement between the present results and the theory in Ref. [7].

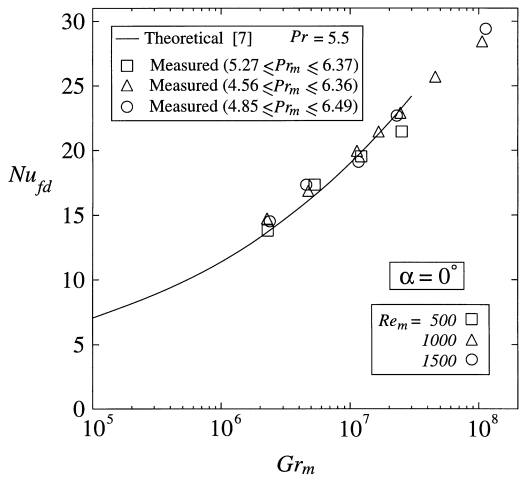

Fig. 9. Comparison between the present data for $\alpha = 0$ and the theoretical predictions in Ref. [7], $Re_m = 500$, 1000, and 1500.

4. Conclusions

The main objective of this investigation was to study the effect of inclination (upward and downward) on the heat-transfer characteristics of laminar mixed convection in semicircular ducts with uniform heat input axially. Water was used as the test fluid and, therefore, only a narrow range of Prandtl number was covered. However, the test matrix for which results were obtained included five orientations ($\alpha = 20°$, 10°, 0°, −10°, and −20°), three Reynolds numbers for each orientation ($Re_m = 500$, 1000, and 1500), and a wide range of Gr_m for each combination of α and Re_m. From these results, the following conclusions can be made:

1. The circumferential variation of wall temperature increases as Gr_m increases for all angles of inclinations. This is attributed to free convective currents that push hot fluid to the upper part of the cross-section and cold fluid to the lower part. Upward inclinations experience less circumferential variation of wall temperature compared to the horizontal orientation at the same Re_m and Gr_m due to the weaker free convective currents within the cross-section. For downward inclinations, the axial variation of wall temperature was found to be strongly dependent on α, Re_m, and Gr_m. At high Gr_m and low Re_m it was not possible to achieve fully-developed temperature profiles within the heated section, possibly due to flow reversal and the accompanying secondary flow loop in the axial flow direction.
2. The axial variation of Nu_z followed the trend noted earlier in Refs. [1,2,4,6] for the horizontal and upward inclinations. Values of Nu_z increased with α

and Gr_m for these orientations. However, the behaviour of Nu_z for downward inclinations was found to be strongly dependent on the combination of Re_m, Gr_m, and α. For $Re_m = 500$ and $\alpha = -20^\circ$, Nu_z was found to decrease continuously with Gr_m, while for $Re_m = 1000$ and 1500, Nu_z may increase and then decrease with Gr_m.

3. Values of Nu_{fd} for the horizontal and upward inclinations (up to $\alpha = 20^\circ$) were found to increase with Gr_m and to be weakly dependent on Re_m. For the downward inclinations, Nu_{fd} was found to be strongly dependent on α, Re_m and Gr_m. These results are consistent in magnitude and trend with the theoretical prediction in [7].

Acknowledgements

The financial assistance provided by the Natural Sciences and Engineering Research Council of Canada is gratefully acknowledged.

References

[1] G.S. Barozzi, E. Zanchini, M. Mariotti, Experimental investigation of combined forced and free convection in horizontal and inclined tubes, MECCANICA 20 (1985) 18–27.

[2] S.M. Morcos, M.M. Hilal, M.M. Kamel, M.S. Soliman, Experimental investigation of mixed laminar convection in the entrance region of inclined rectangular channels, Journal of Heat Transfer 108 (1986) 574–579.

[3] D. Bohne, E. Obermeier, Combined free and forced convection in a vertical and inclined cylindrical annulus, in: Proceedings of the 8th International Heat Transfer Conference, 1986, pp. 1401–1406.

[4] J.R. Maughan, F.P. Incropera, Experiments on mixed convection heat transfer for airflow in a horizontal and inclined channel, International Journal of Heat and Mass Transfer 30 (1987) 1307–1318.

[5] A.S. Lavine, M.Y. Kim, C.N. Shores, Flow reversal in opposing mixed convection flow in inclined pipes, Journal of Heat Transfer 111 (1989) 114–120.

[6] Q.M. Lei, A.C. Trupp, Experimental study of laminar mixed convection in the entrance region of a horizontal semicircular duct, International Journal of Heat and Mass Transfer 34 (1991) 2361–2372.

[7] A.A. Busedra, H.M. Soliman, Analysis of laminar mixed convection in inclined semicircular ducts under buoyancy assisted and opposed conditions, Numerical Heat Transfer, Part A: Applications, in press.

[8] S.J. Kline, F.A. McClintock, Describing uncertainties in single-sample experiments, Mechanical Engineering 75 (1953) 3–8.

[9] R. Moffat, Describing the uncertainties in experimental results, Experimenta Thermal and Fluid Science 1 (1988) 3–17.

[10] Q.M. Lei, A.C. Trupp, Forced convection of thermally developing laminar flow in circular sector ducts, International Journal of Heat and Mass Transfer 33 (1990) 1675–1683.

[11] E.M. Sparrow, A. Haji-Sheikh, Flow and heat transfer in ducts of arbitrary shape with arbitrary boundary conditions, Journal of Heat Transfer 88 (1966) 351–358.